Journal of Thermal Analysis, Vol. 44 (1995) 305-312

NUMERICAL MODELLING OF THE SPIRAL PLATE HEAT EXCHANGER

J. F. Devois, J. F. Durastanti and B. Martin*

ISAT (Superior Institute of Transport and Automobile), 19 rue de l'Oratoire, 58000 Nevers, France

(Received October 4, 1993; in revised form April 23, 1994)

Abstract

The spiral plate heat exchanger (SHE) is widely used in plenty of industrial services in full counter current flow liquid-liquid heat exchange. We have produced a thermal modelling of the heat exchanges in both steady-state and time dependent cases with 2D spiral geometry, allowing computation with different materials, forced convective heat transfer models in turbulent flow and geometrical parameters options. We will display here some results in steady-state conditions in order to improve the exchanger performances.

Keywords: finite difference, finite element, plane spiral, thermal exchanger, transient state

Nomenclature

A	Subscript for channel A (hot side)
B	Subscript for channel B (cold side)
c_m	metal wall width /m
e_{flu}	fluid canal spacing /m
S	total exchanger area /m^2
r_{min}	radius of the open center /m
H	exchanger height /m
L	channel length /m
d_H	hydraulic equivalent diameter of a channel section /m
ρ	mass density /$kg\cdot m^{-3}$
C	specific heat /$kJ\cdot kg^{-1}\cdot K^{-1}$
λ	thermal conductivity /$W\cdot m^{-1}\cdot K^{-1}$
μ_w	wall dynamic viscosity of fluid /$N\cdot s\cdot m^{-2}$

* To whom all correspondence should be addressed.

0368–4466/95/ $ 4.00
© 1995 Akadémiai Kiadó, Budapest
John Wiley & Sons, Limited Chichester

μ_f fluid thermal viscosity (middle of the channel) /N·s·m^{-2}
Pr Prandtl number
D mass flow rate /kg·s^{-1}
V average speed /m·s^{-1}
Re Reynolds number
Nu average Nusselt number in turbulent flow
h convective heat transfer coefficient /W·m^{-2}·K^{-1}
T temperature /°C
T_{Ae} input hot temperature (inside) /°C
T_{Be} input cold temperature (outside) /°C
T_{mix} mixture temperature of fluids /°C
ΔT temperature variation input output in the channel /°C

Description of the spiral-plate heat exchanger

The heat exchanger (Fig. 1) is fabricated from two long strips of metal plate which are spaced apart and wound around an open, spilt center to form a pair of concentric spiral passages. Spacing is maintained uniformly along the length of the spiral by spacer studs welded to the plates. The hot fluid enters at the exchangers's center and flows towards the periphery in channel A, the cold fluid enters sideways to lower thermal losses and flows towards the center in channel B (Fig. 2). Channels are folded and welded at their terminations alternatively to give easy access for cleaning, therefore the cross section is not rectangular (Fig. 3).

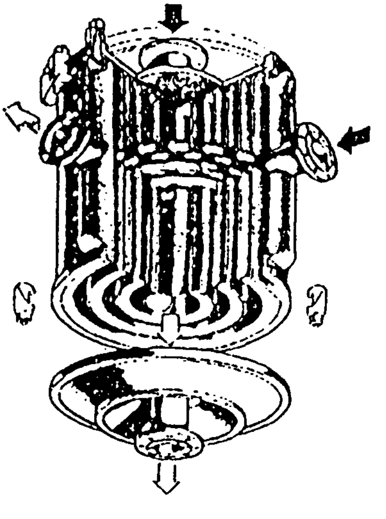

Fig. 1 Spiral heat exchanger SHE1

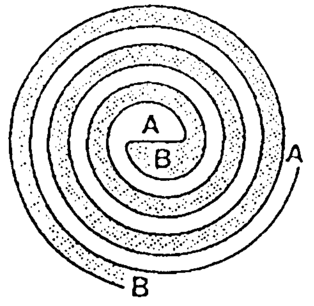

Fig. 2 Spiral plane

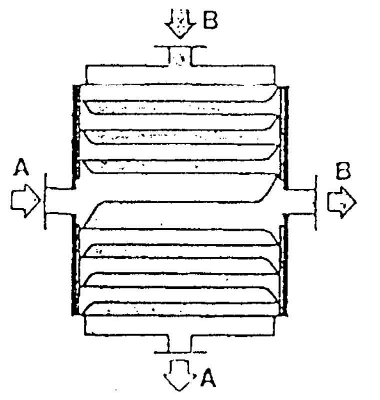

Fig. 3 Axial plane

Equations and thermo-physical parameters

The heat flow is modelled in the direction normal to the metallic walls by conduction and forced convection so that the studs have no influence because they induce some turbulences in the direction normal to the heat flow. The spiral curvature causes turbulences known as Taylor–Gortler phenomenon, which increase the convective heat-transfer coefficient along the metallic wall. With the following hypothesis: incompressible fluids, no internal sources, no dissipation function, neglected longitudinal diffusion, uniform temperature across a channel, fully developed turbulent flow, isotropic metal, we can write heat conservation law [1]:

$$\rho C \frac{\partial T}{\partial t} + \mathrm{div}(\rho C T \vec{V}) = -\,\mathrm{div}(\vec{\Phi}_{qc} + \vec{\Phi}_{qh})$$

where the conductive heat flow inside metal:

$$\vec{\Phi}_{qc} = -\lambda \text{ grad } (T)$$

and the forced convective heat flow at the metal–fluid sublayer boundary:

$$\vec{\Phi}_{qh} = -h(T_{fluid} - T_{wall})$$

The computation of the convective heat transfer coefficient is generally complex because it must take into account additional turbulences caused by the spiral curvature. We have:

$$h = \lambda \frac{Nu}{d_H}$$

The Nusselt number which characterizes the forced convective heat transfer is modelled three ways:

– The standard approach with the Colburn Petrukhov formula:

$$Nu = 0.023 \cdot Re^{0.8} \cdot Pr^{0.333} \left(\frac{\mu_w}{\mu_f}\right)^n$$

with $n=-0.25$ for cooling ($\mu_w > \mu_f$) and $n=-0.11$ for heating ($\mu_w < \mu_f$).

– The local approach which uses the local curvature radius r_c of the channel (Ito) [3]:

$$Nu = 0.021 \cdot Re^{0.85} \cdot Pr^{0.4} \left(\frac{d_H}{2r_c}\right)^{0.1}$$

– The global approach which gives a correction for the exchanger (Baird) [4]:

$$Nu = Pr^{0.25} \left(\frac{\mu_f}{\mu_w}\right)^{0.17} \left[0.0315 \cdot Re^{0.8} - 6.65 \cdot 10^{-7} \left(\frac{L}{e_{flu}}\right)^{1.8}\right]$$

Steady-state numeric discretization

Two different numeric approaches have been realised to model the heat exchanges: finite differences [2] (both steady-state and time dependent cases) and finite elements [5] (only steady-state). We will describe in this paper only the finite difference method being used in steady-state operation. The main problem in modelling is the particular geometry which imposes a netting by regular sectors (Fig. 5), the minimal amount of sectors by turn is imposed by the computing accuracy; the number of nodes increases quickly as the number of turns raises; so we must find a minimal numerical system to get an operative model: robust and accurate but quick enough to be used in interactive CAO design work. The Fig. 4 displays the spatial temperature discretization:

$T_1(\Theta)$ = internal temperature of the first metal wall
$T_2(\Theta)$ = external temperature of the first metal wall
$T_3(\Theta)$ = average temperature of fluid A = T_A
$T_4(\Theta)$ = internal temperature of the second metal wall
$T_5(\Theta)$ = external temperature of the second metal wall
$T_6(\Theta)$ = average temperature of fluid B
$T_7(\Theta) = T_1(\Theta + 2\pi)$
$T_8(\Theta) = T_2(\Theta + 2\pi)$
$T_9(\Theta) = T_3(\Theta + 2\pi)$
$T_0(\Theta) = T_6(\Theta + 2\pi)$

Using pseudo-periodicity of the sectorial mesh we have

$$K_{tA}\left(\frac{dT_3}{d\theta}\right) = c_{30}T_o + c_{33}T_3 + c_{36}T_6$$

$$K_{tB}\left(\frac{dT_6}{d\theta}\right) = c_{63}T_3 + c_{66}T_6 + c_{69}T_9$$

with

$$K_{tA} = \frac{(D_A C_A)}{Hh_A} \quad \text{and} \quad K_{tB} = -\frac{(D_B C_B)}{Hh_B}$$

The c_{ij} factors are functions of local h_A and h_B, metal equivalent $h_e = \lambda_{metal}/e_m$, and curvatures radiuses (Fig. 4).

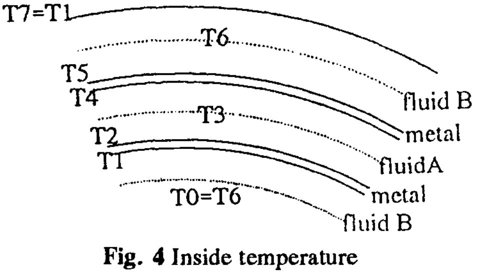

Fig. 4 Inside temperature

The derivate form $dT/d\Theta$ is discretized by classic Crank-Nicholson method for a $\Delta\Theta$ sector angle; $T_{i,n}$ for the Θ angle and $T_{i,n-1}$ for $\Theta - \Delta\Theta$ angle and $T_{i,n+1}$ for the $\Theta + \Delta\Theta$ angle

$$\frac{dT}{d\Theta} = \tau \frac{(T_{n+1} - T_n)}{\Delta\Theta} + (1 - \tau) \frac{(T_n - T_{n-1})}{\Delta\Theta} \qquad 0 < \tau < 1$$

this gives us two recurrent numerical equations for a number of sectors equal to NF

$$T_{3,n+1} = \left(\frac{\Delta\Theta}{\tau K_{tA}}\right)(c_{30}T_{o,n} + c_{33}T_{3,n} + c_{36}T_{6,n}) - \frac{(1 - 2\tau)}{\tau} T_{3,n} + \frac{(1 - \tau)}{\tau} T_{3,n-1}$$

$$T_{6,n-1} = \left(\frac{\tau}{1 - \tau}\right) T_{6,n+1} + \frac{(1 - 2\tau)}{(1 - \tau)} T_{6,n} - \left(\frac{\Delta\Theta}{(1 - \tau)K_{tB}}\right)(c_{63}T_{3,n} + c_{66}T_{6,n} + c_{69}T_{9,n})$$

with Dirichlet boundary conditions: $T_{3,0}=T_{Ae}$, $T_{6NF}=T_{Be}$ and $T_{environ}$ on the external boundary. This crosswise structure for iterations has been used to speed the computer convergence of calculations. We use a ping-pong strategy for thermo-physical parameters variations with temperature profiles: we freeze parameters to compute the temperature and then we refresh parameters with the new temperatures, and this until the end of numerical variations of temperature.

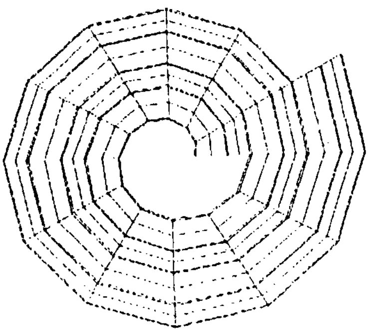

Fig. 5 Spiral mesh (12 sectors/turns)

Validation and results

The validation of the numerical model scheme has been made by comparison with the analytical model of the straight plane exchanger with constant parameters and with a straight geometry for discretization processing. We obtain, if $\tau>0.6$, a stable and accurate output with a great computing speed for this minimal model.

With the complete model our results fit well with Alfa-Laval data. We use Fig. 6 all computing options on an example of parameter sensitivity to improve the exchanger design. We have a water/AISI304/water exchanger with $D_A=D_B$.

The analytical results of the straight plane exchanger give us a simple way to compute the exchanger area (S heat transfer area):

$$S = \left(\frac{DC}{h_g}\right)\left(\frac{\varepsilon}{1-\varepsilon}\right)$$

where the efficiency of the straight plate exchanger:

$$\varepsilon = \frac{\Delta T}{T_{Ae} - T_{Be}}$$

and h_g global heat transfer coefficient:

$$\frac{1}{h_g} = \frac{1}{h_A} + \frac{e_m}{\lambda} + \frac{1}{h_B}$$

We will use the S area to compare the efficiency computed with different physical models in function of the average fluid speed. With a required variation of temperature on a channel ΔT equal to 35 deg; we adjust the S area with speed variations. Using the Colburn formula at mixture temperature we compute the global exchange factor h_g; with $\varepsilon = 35/50°C$ imposed, we obtain the area S of the straight plane exchanger, that we use as thermal exchange area by approximation. The analytical curve Fig. 6 is spiral geometry with temperature constant thermo-physical parameters, it can be compared to the Colburn model. We have a good agreement between global Baird model and local Ito model: both curves have a maximum; but when the optimum for Baird model is under 1 m/s, it is 3 m/s for local model just over the standard use range (0.5 m/s to 2.5 m/s). We can recommend an increase of the fluid speed just over that stan-dard range; if

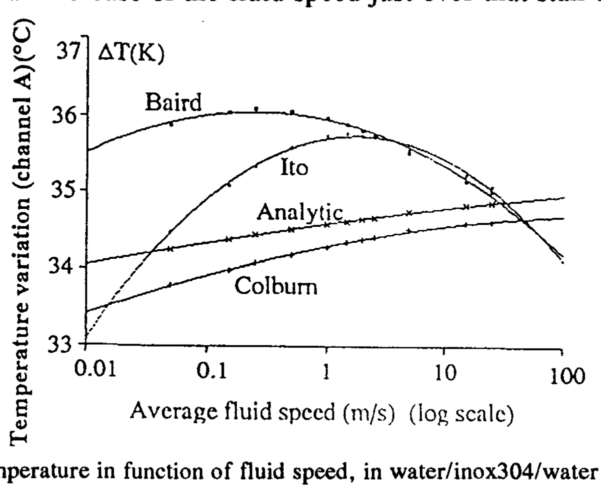

Fig. 6 Temperature in function of fluid speed, in water/inox304/water system

the pressure drop in the exchanger which increases with V^2 can be afforded. We can notice that under 2 m/s the global Baird model overestimate heat transfer compared with local Ito model. And a difference of 1 deg between models causes a relative variation of 2.8% in efficiency around 35°C but as we have for the analytical straight model:

$$\frac{\Delta\varepsilon}{\varepsilon} = (1 - \varepsilon)\,\frac{\Delta S}{S}$$

it will cause a 9.4% relative variation in heat transfer area to obtain the same 70% efficiency.

Conclusion

This example shows how this operative model is a useful and efficient tool to improve conception and design of spiral heat exchangers. With a material library, its spiral *2D* geometry, its curvature radius and channel ends foldings, it allows a more precise knowledge of thermal exchanges inside the exchanger. Only a full three-dimensional, fluid-mechanics computing model taking into account spiral geometry, channel foldings and studs local influences would permit to go further, but it will require computing resources on too large a scale, on grid size and computing power, for our minimal operative approach.

References

1 Incropera and de Witt, Fundamentals of heat and mass transfer, Wiley ed., (1990).
2 J. F. Durastanti, Modélisation d'un système thermique complexe: la centrale THEK 2, Thèse de doctorat de l'Université de Provence, (1985).
3 Ito, Friction factors for turbulent flow in curved pipes, Trans. ASME, 81, (1959).
4 Baird, Mc Crae, Rumford and Slesser, Some considerations on heat transfer in spiral heat exchangers, Chem. Eng. Sci., 7, 1 and 2, (1957).
5 Zienkiewicz and Morgan, Finite elements and approximation, Wiley ed., (1983).

Zusammenfassung — Spiralwärmetauscher (SHE) werden auf breitem Gebiet bei einer Vielfalt von industriellen Anwendungen als Flüssigkeits-Flüssigkeits-Wärmetauscher im Gegenstromprinzip eingesetzt. Es wurde sowohl für den Gleichgewichtszustand als auch für zeitabhängige Fälle ein thermisches Modell des Wärmeaustauschers mit 2D-Spiralengeometrie, unter Zulassung der Berechnung mit unterschiedlichen Materialien, mit Modellen für den erzwungenen konvektiven Wärmetransport in turbulenten Strömungen und geometrischen Parameteroptionen erstellt. Vorliegend sollen einige Resultate bei Gleichgewichtsbedingungen dargelegt werden, um die Austauscherfunktion zu verbessern.